

# Thermodynamic properties and coherent states for the harmonic oscillator in cosmic string space-time with dislocation

M. Salazar-Ramírez<sup>a</sup>, R. D. Mota<sup>b</sup>, M. R. Cordero-López<sup>a</sup> and S. de J. Guatemala Marín<sup>a</sup>

<sup>a</sup>*Escuela Superior de Cómputo, Instituto Politécnico Nacional,*

*Av. Juan de Dios Bátiz esq. Av. Miguel Othón de Mendizábal,*

*Col. Lindavista, Alc. Gustavo A. Madero, 07738, Ciudad de México, México,*

*e-mail: msalzarra@ipn.mx; mcorderol@ipn.mx; sguatemalam1600@alumno.ipn.mx*

<sup>b</sup>*Escuela Superior de Ingeniería Mecánica y Eléctrica, Unidad Culhuacán, Instituto Politécnico Nacional,*

*Av. Santa Ana No. 1000, Col. San Francisco Culhuacán, Alc. Coyoacán, 04430, Ciudad de México, Mexico.*

*e-mail: rdmotae@yahoo.com.mx*

Received 11 November 2024; accepted 24 January 2025

We study the problem of a quantum harmonic oscillator in the presence of a repulsive inverse-square potential within a cosmic string space-time that contains a dislocation. Also, we study how a rotational frame affects the quantum harmonic oscillator plus the repulsive potential within this space-time geometry. For both problems, we find three operators for the radial part of each problem and show that they close the  $su(1, 1)$  Lie algebra. From the theory of unitary irreducible representations of the  $su(1, 1)$  Lie algebra, we obtain the energy spectrum from an algebraic point of view. Also, we obtain the wave functions, the radial coherent states, and their time evolution. Finally, we calculate the thermodynamic properties for each of these problems.

*Keywords:* Algebraic methods; coherent states; cosmic string spacetime; quantum statistical physics; Schrödinger factorization.

DOI: <https://doi.org/10.31349/RevMexFis.71.031701>

## 1. Introduction

Cosmic strings are hypothetical objects known in the literature as topological defects that significantly modify the geometrical properties of space-time and that were formed in the early stages of the universe by abrupt energy changes. Other types of defects include domain walls, global monopoles, dislocations and branes. Topological defects have been extensively studied in quantum theory because they alter the particle energy spectrum and wave functions [1–4], depending on whether they have spin zero, spin 1/2, or spin one.

The quantum harmonic oscillator is one of the most extensively investigated systems in the field of quantum mechanics, employing a number of potentials in both relativistic and non-relativistic contexts with spin and pseudospin symmetry [5–7]. Recently, the system has been investigated in the context of interactions with topological defects [8–17]. Faizuddin Ahmed and Abdelmalek Bouzenada study a special Einstein-Maxwell solution. It is characterized by a magnetic field and a positive non-zero cosmological constant. In the context of this magnetic space-time background, they focus on the relativistic dynamics of quantum oscillating fields in the framework of position-dependent mass systems [12]. In Ref. [17], the authors investigated the behavior of a 2D harmonic oscillator embedded in an elastic medium containing a spiral dislocation (or edge dislocation). In that paper an analytical solution for the Schrödinger equation describing the oscillator under the influence of this dislocation is presented. The equivalent of the Aharonov-Bohm effect for bound states within a relativistic quantum system described

by the Klein-Gordon oscillator has been studied in the space-time of a cosmic string with a spacelike dislocation [15]. In a cosmic string background space-time characterized by a stationary cylindrical metric, the generalized relativistic Duffin-Kemmer-Petiau (DKP) oscillator for a spin-zero field was studied in Ref. [16] and its eigenfunctions and its energy spectrum were obtained. Also, in Ref. [16], the radial wave functions for the linear, Coulomb (and shifted Coulomb) and the Cornell potential were found.

The introduction of a quantum oscillator into a cosmic string space-time leads to the appearance of modified energy levels that depend on the parameters that characterize the cosmic string. As a consequence, thermal properties such as partition function, free energy, entropy and specific heat are altered, since these properties depend on the energy levels of the system. In other words, the presence of a cosmic string causes additional terms to appear in the energy spectrum. These terms are associated with the string's tension and the angular deficit it causes. These changes are crucial for understanding how the oscillator behaves at different temperatures and how it exchanges energy with its environment [18, 19].

It has been demonstrated that the energy spectrum of the harmonic oscillator is influenced by the presence of a repulsive inverse-square potential,  $V(r) = 1/r^2$ , which modifies the effective potential experienced by the particle. This results in alterations to the wave functions and energy levels, as well as modifications to the quantization conditions. A number of theoretical studies have demonstrated the potential of rotational frames to significantly influence the behavior of a harmonic oscillator within a given space-time geom-

etry. In particular, these investigations indicate that such effects can be observed when defects such as cosmic strings are taken into account. This influence can be observed in a number of different areas, including the introduction of fictitious forces, additional coupling terms, modifications in the effective potential, energy corrections, and altered equations of motion [20, 21].

Systems with an inverse quadratic potential display greater resistance to fluctuations in temperature. They are capable of absorbing and dissipating energy with minimal changes in temperature, which enhances their stability and resistance to fluctuations in their environment. Consequently, the inverse quadratic potential present in the oscillator Hamiltonian modifies the energy spectrum and density of states in the space-time of cosmic strings. These modifications influence how specific heat capacity responds to changes in temperature [22].

Coherent states exhibit distinctive characteristics. These states behave in a manner analogous to classical particles, exhibiting well-defined position and momentum. They evolve in time in a straightforward manner under the dynamics of the harmonic oscillator. Coherent states are employed as a quantum analogue of classical states, rendering them a pivotal tool in quantum optics, quantum information theory, and quantum computing [23, 24].

Recently, there is a great interest in thermodynamic properties of quantum systems, since they are crucial for developing quantum computing [25–27]. To this respect there is an increasing interest in understanding the thermodynamic properties of fermionic particles, since the acquisition of quantum memory relies on pairing a group of particles, which can be described using thermodynamic principles [28]. In several works the thermodynamic properties for different quantum systems have been studied [19, 29–37]. A. Bouzenada et al. study the thermodynamic properties of the 2D Klein-Gordon resonator in the presence of the cosmological string in the applied magnetic field. For different parameters of the problem, the results are presented as a function of temperature and applied magnetic field [19]. In Ref. [29] the energy and entropies are calculated, and the differences between ensembles in the system of independent harmonic oscillators with the same frequency are clarified in the Tsallis statistics with escort average.

Thermodynamic properties and relativistic behavior of a neutral spin one boson particle in one-dimensional space have also been studied by means of the generalized Duffin-Kemmer-Petiau equation with a new non-minimal coupling related to the  $q$ -deformed formalism [30]. The Dirac equation in  $3 + 1$  dimensional space-time with non-minimal coupling to a linear radial three-vector potential and in the presence of a static electromagnetic potential that represent both the Aharonov-Bohm and magnetic monopole field has been studied [31]. In that Ref. the authors obtained the partition function describing the statistical properties of the system, the mean energy, the Helmholtz free energy, the entropy and the specific heat. In the framework of the Dunkl-Wigner

quantum mechanics, the thermodynamic properties for the generalized Dunkl oscillator were reported in Ref. [32].

The introduction of the dislocation parameter within cosmic string space-time results in a transformation of the topology of space-time. This alteration impacts upon the density of states of the system, modifying the partition function, which consequently affects the rest of the thermodynamic characteristics of the system [38, 39].

In order to preserve quantum coherence, quantum computing devices must be operated at extremely low temperatures. Furthermore, the thermodynamic properties of systems containing topological defects can influence both the energy consumption and thermal management of quantum computing hardware. Efficient thermal management is therefore a crucial factor in the scaling up of quantum computers and in ensuring their practical viability [40, 41].

To gain a deeper understanding of the evolution of coherent states within the harmonic oscillator in space-time, it is crucial to integrate relativistic elements and space-time curvatures into the conventional quantum mechanical framework. This approach provides novel equations, damping factors, and phases that enhance the comprehension of the behavior of quantum systems within complex environments [42].

The purpose of the present work is the study of the harmonic oscillator in cosmic string space-time with dislocation under a repulsive  $1/r^2$  potential and rotational frame, using a strictly algebraic method. Using our method, the energy spectrum and eigenfunctions can be obtained in a more practical way. We also obtain their coherent states and time evolution, as well as their thermodynamic properties, for the cases where there are no defects in the cosmic strings and for zero dislocation parameter.

Our main motivation for studying the quantum harmonic oscillator under a repulsive inverse quadratic potential in cosmic string space-time with dislocation in both inertial and rotational frames is to demonstrate that this problem can be approached from a different perspective, namely by employing factorization methods of quantum mechanics. This approach can help us to show that the radial part of the problem exhibits  $SU(1, 1)$  symmetry, allowing us to derive operators that close the Lie algebra associated with this symmetry. With the help of the representation theory for this algebra, we intend to obtain the energy spectrum and show that it agrees with the results found in the literature [21].

Our second motivation is to obtain information about the modifications that the energy spectrum, wave functions, coherent states, and their time evolution, as well as the thermodynamic properties, may undergo with the inclusion of the parameters  $\alpha$  and  $\chi$ , under the influence of the inverse quadratic repulsive potential and the rotational frame. According to our research, this would be a novel contribution to the literature, particularly in the context of coherent states and thermodynamic properties.

The structure of the work is as follows. In Section 2. The uncoupled differential equations are obtained for the har-

monic oscillator in the topological defect under the repulsive  $1/r^2$  potential. In Section 3, we apply the Schrödinger factorization to the second-order radial differential equation. With the aid of this factorization, we construct three operators that close the  $su(1, 1)$  Lie algebra. By applying the theory of irreducible unitary representations associated with this algebra, we obtain the energy spectrum and the eigenfunctions. Also, these results are particularized for the case where the dislocation parameter  $\chi \rightarrow 0$  and for the case where no cosmic string defect exists  $\alpha \rightarrow 1$ . In Section 4, results similar to those in Section 3 are obtained for the harmonic oscillator in a topological defect under the repulsive  $1/r^2$  potential and considering rotational frame effects. Furthermore, using the Sturmian basis of the  $su(1, 1)$  Lie algebra, the coherent Perelomov states and their time evolution are constructed for the radial equations of both problems. In Section 5 we calculate thermodynamic functions for the two oscillator cases, such as the partition function, the Helmholtz free energy, the mean energy, the entropy, the heat capacity, and the Massieu function. These properties are also particularized for the limits of zero dislocation parameter  $\chi \rightarrow 0$  and no cosmic string defect  $\alpha \rightarrow 1$ . Finally, we give some concluding remarks.

## 2. Harmonic oscillator in topological defect under repulsive $1/r^2$ potential effects

The space-time of the cosmic string with a dislocation is described by the line element [21]

$$ds^2 = -dt^2 + dr^2 + (\alpha^2 r^2 + \chi^2) d\varphi^2 + 2\chi d\varphi dz + dz^2, \quad (1)$$

where  $t \in \mathbb{R}$  is the time coordinate,  $r, \varphi, z$  the cylinder coordinates in  $\mathbb{R}^3$  with a range of values  $r \in \mathbb{R}^+$ ,  $\varphi \in [0, 2\pi\alpha]$ ,  $z \in \mathbb{R}$ ,  $\alpha = (1 - 4\mu)$  represents the cosmic string parameter and runs in the interval  $(0, 1]$  and  $\mu$  is the linear mass density of the string and  $\hbar = 1$ ,  $c = 1$ . The dislocation parameter,  $\chi$  is a positive quantity, considering a linear deformation ("torsion" or "displacement") of space, is defined as the modulus of the Burgers vector  $\vec{b} = b\vec{e}_z$ , which is assumed to be in the  $z$ -direction, thus yielding  $\chi = b/2\pi$ . This Burgers vector defines a line defect. It is essentially a screw dislocation, in which a complete rotation about the  $z$ -axis causes a translation by  $b$  in the  $z$ -direction. It is crucial to remember that because  $b$  is any real number [43]. The metric tensor for the space-time (1) is

$$g_{ij}(x) = \begin{pmatrix} -1 & 0 & 0 & 0 \\ 0 & 1 & 0 & 0 \\ 0 & 0 & \alpha^2 r^2 + \chi^2 & \chi \\ 0 & 0 & \chi & 1 \end{pmatrix}, \quad (2)$$

and its inverse

$$g^{ij}(x) = \begin{pmatrix} -1 & 0 & 0 & 0 \\ 0 & 1 & 0 & 0 \\ 0 & 0 & \frac{1}{\alpha^2 r^2} & -\frac{\chi}{\alpha^2 r^2} \\ 0 & 0 & -\frac{\chi}{\alpha^2 r^2} & 1 + \frac{\chi^2}{\alpha^2 r^2} \end{pmatrix}. \quad (3)$$

The equation

$$\left[ -\frac{1}{2M} \frac{1}{\sqrt{-g}} (\partial_i (\sqrt{-g} g^{ij} \partial_j) + V(r)) \right] \Psi = i \frac{\partial \Psi}{\partial t}, \quad (4)$$

represents the wave equation in covariant form, which takes into account the potential  $V(r)$ , where  $g_{ij}$  is the metric tensor and  $g^{ij}$  its inverse given by the Eqs. (2) and (3), and  $g = \det(g_{ij})$  [44–46]. Thus, the Hamiltonian operator of the HORP has the following form

$$\hat{H}_{osc} = -\frac{1}{2M} \frac{1}{\sqrt{-g}} \partial_i (\sqrt{-g} g^{ij} \partial_j) + \frac{1}{2} M \omega^2 r^2, \quad (5)$$

where  $M$  is the mass of the particle and  $\omega$  is its angular frequency. The eigenvalues equation for the HORP under the influence of a potential  $V(r)$  is given by

$$(\hat{H}_{HORP} + V(r)) \Psi = E \Psi. \quad (6)$$

Now considering an inverse quadratic repulsive potential given by

$$V(r) = \frac{\eta}{r^2}, \quad (7)$$

with  $\eta$  an arbitrary constant,  $\eta > 0$ . Thus, by using Eqs. (5) and (7) the eigenvalue Eq. (6) for the harmonic oscillator in the space-time background can be expressed as [21]

$$-\frac{1}{2M} \left[ \frac{d^2}{dr^2} + \frac{1}{r} \frac{\partial}{\partial r} + \frac{1}{\alpha^2 r^2} \left( \frac{\partial}{\partial \varphi} - \chi \frac{\partial}{\partial z} \right)^2 + \frac{\partial^2}{\partial z^2} \right] \Psi + \left( \frac{1}{2} M \omega^2 r^2 + \frac{\eta}{r^2} \right) \Psi = E \Psi. \quad (8)$$

The initial term on the left-hand side corresponds to the kinetic energy of the system, where the deficit angle of the cosmic string  $\Delta\varphi$  is incorporated, modifying the angular component. Subsequently, the dislocation parameter is introduced into this same energy, leading to a coupling between the angular and longitudinal motions.

By taking into account that the potential we are considering depends only on the radial coordinate  $r$ , the wave function  $\Psi(r, \varphi, z)$  is written as [21]

$$\Psi(r, \varphi, z) = R(r) e^{i\ell\varphi} e^{ikz}. \quad (9)$$

This wave function is dependent on the spatial coordinates. However, the angular component undergoes modification due to the altered topology of the space-time around the cosmic string. Specifically, the presence of an angular deficit  $\Delta\varphi = 2\pi(1-\alpha)$  leads to a substantial alteration in the behavior of the angular coordinate  $\varphi$ . Consequently,  $\varphi$  no longer spans the conventional range of  $2\pi$ , but instead covers a reduced angular range of  $2\pi\alpha$ , where  $\alpha < 1$ . This reduction modifies the periodicity condition, which now takes the form  $e^{i\ell(\varphi+2\pi\alpha)} = e^{i\ell\varphi}$ .

The eigenvalues for the orbital quantum operator are  $\ell = 0, 1, 2, \dots$ , and  $k > 0$  is an arbitrary constant. Therefore, substituting Eqs. (9) into (8), we obtain the following second order differential equation for the radial function  $R(r)$  [21]

$$\frac{d^2 R}{dr^2} + \frac{1}{r} \frac{dR}{dr} + \left[ \lambda - M^2 \omega^2 r^2 - \frac{\tau^2}{r^2} \right] R = 0, \quad (10)$$

where

$$\begin{aligned} \lambda &= 2ME - k^2, & \tau &= \sqrt{\ell_0^2 + 2M\eta}, \\ \ell_0 &= \frac{|\ell - \chi k|}{\alpha}. \end{aligned} \quad (11)$$

Now, we are in the position to obtain the generators of the algebra  $su(1, 1)$ , which are obtained in the next section.

### 2.1. Exact solution from an algebraic method

In this section, we obtain the exact solution of the HORP. For this purpose, we rewrite Eq. (10) as

$$-r^2 \frac{d^2 R}{dr^2} - r \frac{dR}{dr} + M^2 \omega^2 r^4 R - \lambda r^2 R = -\tau^2 R. \quad (12)$$

To solve this equation, we proceed to eliminate the first order derivative by making the variable change  $R = (1/\sqrt{r})G$ . We obtain

$$\left( -r^2 \frac{d^2}{dr^2} + M^2 \omega^2 r^4 - \lambda r^2 \right) G = \left( \frac{1}{4} - \tau^2 \right) G. \quad (13)$$

Now the generators of the  $su(1, 1)$  Lie algebra can be constructed proposing the following factorization for Eq. (13)

$$\left( r \frac{d}{dr} + \Gamma r^2 + \Pi \right) \left( -r \frac{d}{dr} + \Lambda r^2 + \Upsilon \right) G = \Phi G, \quad (14)$$

by developing the left-hand side of this equation and comparing it with Eq. (13), we find that

$$\begin{aligned} \Gamma = \Lambda &= \pm M\omega, \quad \Pi = \Upsilon = -\frac{\lambda}{2M\omega} - 1, \\ \Phi &= \left( \frac{\lambda}{2M\omega} + 1 \right)^2 - \tau^2. \end{aligned} \quad (15)$$

Thus, we can rewrite Eq. (13) as follows

$$(\mathbb{R}_{\mp} \mp 1) \mathbb{R}_{\pm} = \frac{1}{4} \left( \left( \frac{\lambda}{2M\omega} \pm 1 \right)^2 - \tau^2 \right), \quad (16)$$

where the two operators  $\mathbb{R}_+$  and  $\mathbb{R}_-$  are given by

$$\mathbb{R}_{\pm} = \frac{1}{2} \left( \mp r \frac{d}{dr} + M\omega r^2 - \frac{\lambda}{2M\omega} \mp 1 \right). \quad (17)$$

Equations (13) and (17) allow us to define the following operators

$$\mathfrak{S}_{\pm} = \frac{1}{2} \left[ \mp r \frac{d}{dr} + M\omega r^2 \mp 1 \right] - \mathfrak{S}_3, \quad (18)$$

where the third operator  $\mathfrak{S}_3$  is written as

$$\begin{aligned} \mathfrak{S}_3 G &= \frac{1}{4M\omega} \left( -\frac{d^2}{dr^2} + \frac{\tau^2 - \frac{1}{4}}{r^2} + M^2 \omega^2 r^2 \right) G \\ &= \frac{\lambda}{4M\omega} G. \end{aligned} \quad (19)$$

Therefore, it is straightforward to show that the operators  $\mathfrak{S}_+$ ,  $\mathfrak{S}_-$ , and  $\mathfrak{S}_3$  close the  $su(1, 1)$  Lie algebra

$$[\mathfrak{S}_3, \mathfrak{S}_{\pm}] = \pm \mathfrak{S}_{\pm}, \quad [\mathfrak{S}_-, \mathfrak{S}_+] = 2\mathfrak{S}_3. \quad (20)$$

The Casimir operator  $\mathfrak{C}^2$  can be calculated with the help of the operators given in Eqs. (18) and (19), that is

$$\begin{aligned} \mathfrak{C}^2 G &\equiv \mathfrak{S}_3^2 G - \frac{1}{2} (\mathfrak{S}_+ \mathfrak{S}_- + \mathfrak{S}_- \mathfrak{S}_+) G \\ &= [\tau^2 - 1] G. \end{aligned} \quad (21)$$

Using this last equation and Eq. (A.5) of the Appendix, we have

$$[\tau^2 - 1] G = k(k - 1)G. \quad (22)$$

Therefore, we obtain the following relationships

$$k = \frac{1}{2}\tau + \frac{1}{2}, \quad n = n_r, \quad n_r + k = n_r + \frac{1}{2}\tau + \frac{1}{2}, \quad (23)$$

where  $n_r = 0, 1, 2, \dots$

From Eqs. (11), (19), (23) and Eq. (A.4) of the Appendix, we obtain

$$\frac{E}{2\omega} - \frac{k^2}{4m\omega} = n_r + \frac{1}{2}\tau + \frac{1}{2}. \quad (24)$$

Thus, from this relationship, the energy spectrum for the harmonic oscillator in topological defect under repulsive  $1/r^2$  potential effects is

$$E_{n_r, \ell, k} = \frac{k^2}{2M} + \omega [2n_r + 1 + \mathfrak{S}]. \quad (25)$$

If we define  $\rho^2 = M\omega r^2$ , Eq. (13) takes the form

$$\left( \frac{d^2}{d\rho^2} + \frac{\frac{1}{4} - \tau^2}{\rho^2} - \rho^2 + \frac{\lambda}{M\omega} \right) F = 0. \quad (26)$$

On the other hand, it is known that the differential equation [48]

$$y'' + \left[ 4n_r + 2\beta + 2 - x^2 + \frac{\frac{1}{4} - \beta^2}{x^2} \right] y = 0, \quad (27)$$

has as solution [48, 56]

$$y = N_{n_r} e^{-\frac{x^2}{2}} x^{\alpha + \frac{1}{2}} L_{n_r}^{\alpha} (x^2). \quad (28)$$

Equations (27) and (28) can be used to determine the wave functions  $F(r)$  of Eq. (25), yielding to

$$F(r) = \frac{2\Gamma(n_r + 1)}{\Gamma(n_r + \tau + 1)} e^{-\frac{M\omega r^2}{2}} (M\omega)^{\frac{\tau + \frac{1}{2}}{2}} \times r^{\tau + \frac{1}{2}} L_{n_r}^\tau(M\omega r^2). \quad (29)$$

In terms of the group indices  $n$  and  $k = (\tau/2) + (1/2)$ , the Sturmian basis for the irreducible unitary representation of the  $su(1, 1)$  Lie algebra for the HORP is

$$R(r) = \left[ \frac{2\Gamma(n_r + 1)}{\Gamma(n_r + 2k)} \right]^{\frac{1}{2}} \times e^{-\frac{M\omega r^2}{2}} (M\omega)^{\frac{\tau + \frac{1}{2}}{2}} r^\tau L_{n_r}^\tau(M\omega r^2), \quad (30)$$

here the normalization coefficient  $N_n$  was computed from the orthogonality of the Laguerre polynomials. The particular cases of our general results obtained above in this section are given in the next section.

## 2.2. Particular cases solutions for $V(r) = 0$ , $\chi \rightarrow 0$ and $\alpha \rightarrow 1$

When there is no external potential present  $V(r) = 0$ , that is  $\eta \rightarrow 0$ , the Sturmian basis and the energy eigenvalues for the HORP are given by

$$R(r) = \left[ \frac{2\Gamma(n_r + 1)}{\Gamma(n_r + 2k)} \right]^{\frac{1}{2}} e^{-\frac{M\omega r^2}{2}} (M\omega)^{\frac{|\ell - \chi k| + \frac{1}{2}}{2}} \times r^\tau L_{n_r}^{|\ell - \chi k|}(M\omega r^2), \quad (31)$$

and

$$E_{n_r, \ell, k} = \frac{k^2}{2M} + \omega \left[ 2n_r + 1 + \frac{|\ell - \chi k|}{\alpha} \right]. \quad (32)$$

For zero dislocation parameter  $\chi \rightarrow 0$ , the Sturmian basis and the energy eigenvalues for the HORP are

$$R(r) = \left[ \frac{2\Gamma(n_r + 1)}{\Gamma(n_r + 2k)} \right]^{\frac{1}{2}} \times e^{-\frac{M\omega r^2}{2}} (M\omega)^{\frac{\Xi + \frac{1}{2}}{2}} r^\Xi L_{n_r}^\Xi(M\omega r^2), \quad (33)$$

and

$$E_{n_r, \ell, k} = \frac{k^2}{2M} + \omega [2n_r + 1 + \Xi], \quad (34)$$

where  $\Xi = \sqrt{(\ell^2/\alpha^2) + 2M\eta}$ . With no cosmic string defect,  $\alpha \rightarrow 1$ , the Sturmian basis and the energy eigenvalues for HORP are given by

$$R(r) = \left[ \frac{2\Gamma(n + 1)}{\Gamma(n + 2k)} \right]^{\frac{1}{2}} \times e^{-\frac{M\omega r^2}{2}} (M\omega)^{\frac{\Upsilon + \frac{1}{2}}{2}} r^\Upsilon L_n^\Upsilon(M\omega r^2), \quad (35)$$

and

$$E_{n, \ell, k} = \frac{k^2}{2M} + \omega [2n + 1 + \Upsilon], \quad (36)$$

respectively, and  $\Upsilon = \sqrt{(\ell - \chi k)^2 + 2M\eta}$ . The results presented in this subsection, derived using this methodology, are in accordance with those reported by Ref [21].

## 3. Harmonic oscillator in topological defect under repulsive $1/r^2$ potential and rotational frame effects

In this section, we study the influence of the rotational frame on the harmonic oscillator within the same space-time geometry given by Eq. (1) with a repulsive inverse quadratic potential (HORPRF). Let us begin by performing a coordinate transformation given by  $\varphi = \varphi + \Omega t$ , where  $\Omega$  is the constant angular velocity of the rotating frame. Thus, the line element from Eq. (1) is expressed as [50–53]

$$ds = - (1 - \Omega^2 \alpha^2 r^2) dt^2 + 2\Omega \alpha^2 r^2 d\varphi dt + dr^2 + \alpha^2 r^2 d\varphi^2 + (dz + \chi d\varphi)^2, \quad (37)$$

in this context, the term  $(1 - \Omega^2 \alpha^2 r^2) dt^2$  represents a modification of the time element because of the rotation of the system. As  $r$  increases, the proper time is affected by the rotation in an analogous way to a relativistic effect. The second term  $2\Omega \alpha^2 r^2 d\varphi dt$  in this metric incorporates both time and angular coordinates. This term arises because of the rotation of the system and represents the precession of orbits within the context of rotational space-time. In general relativity, such a term is fundamental to describe phenomena such as the Coriolis force in rotating systems. In the fourth and fifth terms,  $\alpha^2 r^2 d\varphi^2$  and  $(dz + \chi d\varphi)^2$ , respectively, the variable  $\varphi$  continues to show an angular deficit relative to  $\alpha$ .

In a rotational frame, the combination of the dislocation and the rotation effect may cause the particle trajectories to be neither circular nor closed, but to have a more complex precession and a deviation from standard geodesics.

Thus, in the rotating reference frame, the line element (37) allows us to see that the radial coordinate in the cosmic string space-time is restricted to the region

$$0 \leq r < \frac{1}{\Omega \alpha}. \quad (38)$$

If the speed of the particle exceeds that of light, it can be shown that the values of the radial coordinate satisfy  $r > 1/\Omega \alpha$ , which implies that the particle is located outside the light cone [50].

The rotating frame is defined as

$$\vec{\Omega} = \Omega \hat{z}, \quad (39)$$

and therefore the HORPRF has the following Hamiltonian [21]

$$\hat{\mathcal{H}}_{osc} = \hat{H}_{osc} - \vec{\Omega} \cdot \mathbf{L}, \quad (40)$$

where  $\hat{H}_{osc}$  is defined in Eq. (5) and  $\mathbf{L}$  is the angular momentum operator. It is shown that the presence of the dislocation  $\chi$  modifies the  $z$  component of the angular momentum operator for the space-time geometry given in Eq. (1), as follows [4, 49]

$$\hat{L}_z^{eff} = -\frac{i}{\alpha} \left( \frac{\partial}{\partial \varphi} - \chi \frac{\partial}{\partial z} \right) \hat{z}. \quad (41)$$

Thus, the eigenvalue equation for the HORPRF is written as

$$\left[ \hat{\mathcal{H}}_{HORPRF} - V'(r) \right] \Phi = \mathcal{E}_{HORPRF} \Phi. \quad (42)$$

In this case,  $V'(r) = V(r) - V_0$ , where  $V(r)$  indicates a repulsive inverse-square potential as given by Eq. (7) and  $V_0$  is a constant potential term that only shifts the energy. Thus the Hamiltonian given in Eq. (42) for this particular quantum system is given by

$$-\frac{1}{2M} \left[ \frac{d^2}{dr^2} + \frac{1}{r} \frac{\partial}{\partial r} + \frac{1}{\alpha^2 r^2} \left( \frac{\partial}{\partial \varphi} - \chi \frac{\partial}{\partial z} \right)^2 + \frac{\partial^2}{\partial z^2} \right] \Psi + \left( \frac{1}{2} M \omega^2 r^2 + \frac{\eta}{r^2} - V_0 + i \frac{\Omega}{\alpha} \left( \frac{\partial}{\partial \varphi} - \chi \frac{\partial}{\partial z} \right) \right) \Psi = \mathcal{E}_{osc} \Psi. \quad (43)$$

### 3.1. Exact solutions

From Eqs. (9) and (43) we arrive to the differential equation

$$\frac{d^2 R}{dr^2} + \frac{1}{r} \frac{dR}{dr} + \left[ \Lambda - M^2 \omega^2 r^2 - \frac{\tau^2}{r^2} \right] R = 0, \quad (44)$$

where

$$\Lambda = 2M (\mathcal{E}_{HORPRF} + \Omega \ell_0 + V_0) - k^2, \quad (45)$$

and  $\tau$  and  $\ell_0$  are given by Eq. (11). Starting from Eq. (44), we proceed as in Sec. 3 to obtain the exact solution of the HORPRF from an algebraic point of view. Thus, the operators obtained from this factorization method are given by

$$\mathfrak{X}_{\pm} = \frac{1}{2} \left[ \mp r \frac{d}{dr} + M \omega r^2 \mp 1 \right] - \mathfrak{X}_3, \quad (46)$$

where the third operator  $\mathfrak{X}_3$  is written as

$$\begin{aligned} \mathfrak{X}_3 G &= \frac{1}{4M\omega} \left( -\frac{d^2}{dr^2} + \frac{\tau^2 - \frac{1}{4}}{r^2} + M^2 \omega^2 r^2 \right) G \\ &= \frac{\Lambda}{4M\omega} G. \end{aligned} \quad (47)$$

These operators close the  $su(1, 1)$  Lie algebra

$$[\mathfrak{X}_3, \mathfrak{X}_{\pm}] = \pm \mathfrak{X}_{\pm}, \quad [\mathfrak{X}_-, \mathfrak{X}_+] = 2\mathfrak{X}_3. \quad (48)$$

It can be seen that the Casimir operator for this algebra is the same as that of Eq. (21), and therefore the relationship between  $k$  and  $\tau$  is given by Eq. (23). Thus, from Eqs. (47), (23) and Eq. (A.4) of the Appendix, the energy spectrum for HORPRF is given by

$$\begin{aligned} \mathcal{E}_{HORPRF}^{n_r, \ell, k} &= \frac{k^2}{2M} + \omega [2n_r + 1 + \mathfrak{S}] \\ &\quad - \Omega \frac{|\ell - \chi k|}{\alpha} - V_0. \end{aligned} \quad (49)$$

with  $\mathfrak{S} = \sqrt{((\ell - \chi k)^2 / \alpha^2) + 2M\eta}$ . The Sturmian basis for the irreducible unitary representation of the  $su(1, 1)$  Lie algebra, expressed in terms of the group indices  $n$  and  $k = (\tau/2) + (1/2)$  result to be

$$\begin{aligned} R(r) &= \left[ \frac{2\Gamma(n_r + 1)}{\Gamma(n_r + 2k)} \right]^{\frac{1}{2}} e^{-\frac{M\omega r^2}{2}} (M\omega)^{k + \frac{1}{2}} \\ &\quad \times r^{2k-1} L_{n_r}^{2k-1}(M\omega r^2). \end{aligned} \quad (50)$$

It can be seen that it is the same as that calculated in Sec. 3, Eq. (30) and are consistent with those reported by Ref. [21].

For the particular case where the dislocation parameter  $\chi \rightarrow 0$ , the energy spectrum is given by

$$\mathcal{E}_{HORPRF}^{n_r, \ell, k} = -\Omega \frac{|\ell|}{\alpha} + \frac{k^2}{2M} + \omega [2n_r + 1 + \Xi], \quad (51)$$

and the Sturmian basis for this case is the same as that given by Eq. (33) For the case where the cosmic string parameter  $\alpha \rightarrow 1$ , the energy spectrum is given by

$$\mathcal{E}_{HORPRF}^{n, \ell, k} = -\Omega |\ell - \chi k| - \frac{k^2}{2M} + \omega [2n + 1 + \Upsilon], \quad (52)$$

and the Sturmian basis for this case is the same as that of Eq. (35).

## 4. $SU(1, 1)$ radial coherent states and their time evolution for the HORP and HORPRF

We use Perelomov's definition of the  $SU(1, 1)$  coherent states [54] to calculate the coherent states corresponding to the radial functions obtained for the HORP in Sec. 3. That is

$$\begin{aligned} |\zeta\rangle &= \mathfrak{D}(\xi) |k, 0\rangle \\ &= (1 - |\xi|^2)^k \sum_{n=0}^{\infty} \sqrt{\frac{\Gamma(n+2k)}{n! \Gamma(2k)}} \xi^n |k, n\rangle, \end{aligned} \quad (53)$$

where  $\mathfrak{D}(\xi)$  represents the displacement operator, while  $|k, 0\rangle$  denotes the lowest normalized state. Consequently, when we apply the operator  $\mathfrak{D}(\xi)$  to the ground state of the functions  $R(\rho)$ . We obtain

$$\begin{aligned} R(r) &= \left[ \frac{2(1 - |\xi|^2)^{\mathfrak{S}+1}}{\Gamma(\mathfrak{S}+1)} \right]^{\frac{1}{2}} e^{-\frac{M\omega r^2}{2}} (M\omega)^{\frac{\mathfrak{S}+1}{2}} r^{\mathfrak{S}} \\ &\quad \times \sum_{n=1}^{\infty} \xi^2 L_n^{\mathfrak{S}}(M\omega r^2). \end{aligned} \quad (54)$$

The generating function of the Laguerre polynomials

$$\sum_{n=0}^{\infty} L_n^\mu(x) y^n = \frac{e^{-xy/(1-y)}}{(1-y)^{\mu+1}}, \quad (55)$$

can be used to determine the sum of the above equation. Therefore, the radial coherent states  $R(r)$ , can be expressed as

$$R(r) = \left[ \frac{2(1-|\xi|^2)^{\mathfrak{S}+1}}{\Gamma(\mathfrak{S}+1)(1-\xi)^{2\mathfrak{S}+2}} \right]^{\frac{1}{2}} (M\omega)^{\frac{\mathfrak{S}+\frac{1}{2}}{2}} \times r^{\mathfrak{S}} e^{\frac{M\omega r^2}{2} \left( \frac{\xi+1}{\xi-1} \right)}. \quad (56)$$

Thus, for zero dislocation parameter  $\chi \rightarrow 0$  the radial coherent states  $R(r)$  are given by

$$R(r) = \left[ \frac{2(1-|\xi|^2)^{\Xi+1}}{\Gamma(\Xi+1)(1-\xi)^{2\Xi+2}} \right]^{\frac{1}{2}} (M\omega)^{\frac{\Xi+\frac{1}{2}}{2}} \times r^{\Xi} e^{\frac{M\omega r^2}{2} \left( \frac{\xi+1}{\xi-1} \right)}. \quad (57)$$

If no cosmic string defects exists,  $\alpha \rightarrow 1$ , the radial coherent states  $R(r)$  are

$$R(r) = \left[ \frac{2(1-|\xi|^2)^{\Upsilon+1}}{\Gamma(\Upsilon+1)(1-\xi)^{2\Upsilon+2}} \right]^{\frac{1}{2}} (M\omega)^{\frac{\Upsilon+\frac{1}{2}}{2}} \times r^{\Upsilon} e^{\frac{M\omega r^2}{2} \left( \frac{\xi+1}{\xi-1} \right)}. \quad (58)$$

To obtain the time evolution of these coherent states, we now write Eq. (10) as follows

$$H_r G = \lambda G, \quad (59)$$

where

$$H_r = \left( -r^2 \frac{d^2}{dr^2} + \frac{\tau^2 - \frac{1}{4}}{r^2} + M^2 \omega^2 r^2 \right). \quad (60)$$

Therefore, from Eqs. (19) and (59), the following relation can be obtained

$$H_r G = 4M\omega \mathfrak{S}_3 G = \lambda G. \quad (61)$$

Equations (19), (61) and (A.4) of the appendix allow us to recalculate the energy spectrum obtained in Eq. (25) of Sec. 3. We obtain

$$E_{n_r, \ell, k} = \frac{k^2}{2M} + \omega [2n_r + 1 + \mathfrak{S}]. \quad (62)$$

The definition of the time evolution operator for an arbitrary Hamiltonian is [55]

$$\mathcal{U}(t) = e^{-iH_r t/\hbar} = e^{-4iM\omega \mathfrak{S}_3 t/\hbar}. \quad (63)$$

It is considered that  $t$  is a fictitious time [56, 57]. The time evolution of the Perelomov coherent states is defined by

$$|\zeta(\tau)\rangle = \mathcal{U}(t)|\zeta\rangle = \mathcal{U}(t)\mathfrak{D}(\xi)\mathcal{U}^\dagger(\tau)\mathcal{U}(t)|k, 0\rangle, \quad (64)$$

where  $\xi$  is a complex number and  $D(\xi) = \exp(\xi\mathfrak{D}_+ - \xi^*\mathfrak{D}_-)$  is the displacement operator. Thus, the time-dependent Perelomov coherent states can be written as [47]

$$|\zeta(t')\rangle = e^{-4iM\omega k t \hbar} e^{\zeta(t)\mathfrak{D}_+} e^{\eta\mathfrak{D}_0} e^{-\zeta(-t)^*\mathfrak{D}_-} |k, 0\rangle. \quad (65)$$

This result allows us to calculate the time evolution for the HORP. It results to be

$$R(r, \xi) = \left[ \frac{2(1-|\xi|^2)^{\mathfrak{S}+1} (m\omega)^{\mathfrak{S}+\frac{1}{2}}}{\Gamma(\mathfrak{S}+1)(1-\xi e^{4iM\omega\tau/\hbar})^{2\mathfrak{S}+2}} \right]^{\frac{1}{2}} r^{\mathfrak{S}} \times e^{-4iM\omega(\frac{1}{2}\mathfrak{S}+\frac{1}{2})} e^{\frac{M\omega r^2}{2} \left( \frac{\xi e^{4iM\omega\tau/\hbar} + 1}{\xi e^{4iM\omega\tau/\hbar} - 1} \right)}. \quad (66)$$

It is worth mentioning that the coherent states and their time evolution for the HORPRF exhibit the same behavior as Eqs. (56) and (66) due to the use of identical Sturmian bases.

## 5. Thermodynamic properties for HORP and HORPRF

In this section, we calculate the thermodynamic properties for the HORP and HORPRF problems. For each of them, we find the partition function, the Helmholtz free energy, the mean energy, the entropy, the heat capacity, and the Massieu function. Also, we find for some of them the limiting cases for no string defect  $\alpha \rightarrow 1$  and for no dislocation  $\chi \rightarrow 0$ .

### 5.1. Thermodynamic properties for the HORP

It is known that the partition function  $z$  is defined by

$$z = \sum_{n=0}^{\infty} e^{-\beta E_{n_r, \ell, k}}, \quad (67)$$

where  $\beta = 1/kT$ ,  $k$  is the Boltzmann constant and  $T$  the absolute temperature. Thus, from Eqs. (67) and (25) the partition function can be writing as

$$z = \frac{\exp \left[ -\beta \left( \frac{k^2}{2M} + \omega \mathfrak{S} \right) \right]}{2 \sinh \omega \beta}, \quad (68)$$

and the Helmholtz free energy can be calculated as follows

$$F = -\frac{1}{\beta} \ln z = \frac{k^2}{2M} + \omega \mathfrak{S} + \frac{1}{\beta} \ln (2 \sinh \omega \beta), \quad (69)$$

the mean free energy is given by

$$U = -\frac{\partial \ln z}{\partial \beta} = \frac{k^2}{2M} + \omega \mathfrak{S} + \omega \coth \omega \beta, \quad (70)$$

the entropy for this quantum system, can be calculated with the help of Eqs. (68) and (70) as follows

$$S = k \ln z + \frac{U}{T} = k [\omega \beta \coth \omega \beta - \ln (2 \sinh \omega \beta)], \quad (71)$$

the specific heat capacity  $C/k$  is calculated from Eq. (68) as

$$\frac{C}{k} = \beta^2 \left[ \frac{\partial^2 \ln z}{\partial \beta^2} \right] = \frac{\beta^2 \omega^2}{\sinh^2 \omega \beta}. \quad (72)$$

Finally, from Eqs. (70) and (71) the Massieu function can be calculated as

$$f_M = -\frac{U}{T} + S = \frac{k^2}{2MT} + \frac{\omega}{T} [\mathfrak{S} + \coth \omega \beta] + k [\omega \beta \coth \omega \beta - \ln (2 \sinh \omega \beta)]. \quad (73)$$

Now, we particularize some of our results above for the limit cases:  $\mathbb{A}$ ) for no string defect  $\alpha \rightarrow 1$  and  $\mathbb{B}$ ) for no dislocation  $\chi \rightarrow 0$ .

*Case  $\mathbb{A}$ :*

If no cosmic string defects exists,  $\alpha \rightarrow 1$ , the partition function takes the form

$$z = \frac{\exp \left[ -\beta \left( \frac{k^2}{2M} + \omega \Upsilon \right) \right]}{2 \sinh \omega \beta}, \quad (74)$$

the Helmholtz free energy results to be

$$F = \frac{k^2}{2M} + \omega \Upsilon + \frac{1}{\beta} \ln (2 \sinh \omega \beta). \quad (75)$$

The mean free energy is given by

$$U = \frac{k^2}{2M} + \omega \Upsilon + \omega \coth \omega \beta, \quad (76)$$

and finally, the Massieu function under this potential is

$$f_M = \frac{k^2}{2MT} + \frac{\omega}{T} [\Upsilon + \coth \omega \beta] + k [\omega \beta \coth \omega \beta - \ln (2 \sinh \omega \beta)]. \quad (77)$$

*Case  $\mathbb{B}$ :*

If no dislocation exists  $\chi \rightarrow 0$ , our general results above are particularized as follows. The partition function in this limit is given by

$$z = \frac{\exp \left[ -\beta \left( \frac{k^2}{2M} + \omega \Xi \right) \right]}{2 \sinh \omega \beta}, \quad (78)$$

and the Helmholtz free energy takes the form

$$F = \frac{k^2}{2M} + \omega \Xi + \frac{1}{\beta} \ln (2 \sinh \omega \beta). \quad (79)$$

The mean free energy simplifies to

$$U = \frac{k^2}{2M} + \omega \Xi + \omega \coth \omega \beta, \quad (80)$$

and the Massieu function is given by

$$f_M = \frac{k^2}{2MT} + \frac{\omega}{T} [\Xi + \coth \omega \beta] + k [\omega \beta \coth \omega \beta - \ln (2 \sinh \omega \beta)]. \quad (81)$$

## 5.2. Thermodynamic properties for the HORPRF

In this subsection, we obtain the thermodynamic properties for the HORPRF. These are computed beginning with the partition function under rotational frame effects, which takes the form

$$z = \frac{\exp \left[ -\beta \left( \frac{k^2}{2M} + \omega \mathfrak{S} - \Omega \frac{|\ell - \chi k|}{\alpha} - V_0 \right) \right]}{2 \sinh \omega \beta}. \quad (82)$$

Thus, the Helmholtz free energy is given by

$$F = \frac{k^2}{2M} + \omega \mathfrak{S} - \Omega \frac{|\ell - \chi k|}{\alpha} - V_0 + \frac{1}{\beta} \ln (2 \sinh \omega \beta). \quad (83)$$

The mean free energy for this case takes the form

$$U = \frac{k^2}{2M} + \omega \mathfrak{S} - \Omega \frac{|\ell - \chi k|}{\alpha} - V_0 + \omega \coth \omega \beta. \quad (84)$$

The Massieu function result to be

$$f_M = \frac{k^2}{2MT} + \frac{\omega}{T} \left[ \mathfrak{S} - \Omega \frac{|\ell - \chi k|}{\alpha} - V_0 + \coth \omega \beta \right] + k [\omega \beta \coth \omega \beta - \ln (2 \sinh \omega \beta)]. \quad (85)$$

Now, we particularize some of the results (82)-(85) for the cases:  $\mathbb{C}$ )  $\chi \rightarrow 0$ , and  $\mathbb{D}$ )  $\alpha \rightarrow 1$ .

*Case  $\mathbb{C}$ :*

The partition function simplifies to

$$z = \frac{\exp \left[ -\beta \left( \frac{k^2}{2M} + \omega \Xi - \Omega \frac{|\ell|}{\alpha} - V_0 \right) \right]}{2 \sinh \omega \beta}. \quad (86)$$

Thus, the Helmholtz free energy is given by

$$F = \frac{k^2}{2M} + \omega \Xi - \Omega \frac{|\ell|}{\alpha} - V_0 + \frac{1}{\beta} \ln (2 \sinh \omega \beta), \quad (87)$$

and the mean free energy results to be

$$U = \frac{k^2}{2M} + \omega \Xi - \Omega \frac{|\ell|}{\alpha} - V_0 + \omega \coth \omega \beta. \quad (88)$$

The Massieu function under the limit reduces to

$$f_M = \frac{k^2}{2MT} + \frac{\omega}{T} \left[ \Xi - \Omega \frac{|\ell|}{\alpha} - V_0 + \coth \omega \beta \right] + k [\omega \beta \coth \omega \beta - \ln (2 \sinh \omega \beta)]. \quad (89)$$

*Case  $\mathbb{D}$ :*

If no cosmic string defects exists, Eqs. (82)-(85) are particularized as follows. The partition function reduces to

$$z = \frac{\exp \left[ -\beta \left( \frac{k^2}{2M} + \omega \Upsilon - \Omega |\ell - \chi k| - V_0 \right) \right]}{2 \sinh \omega \beta}. \quad (90)$$

Therefore, the Helmholtz free energy is given by

$$F = \frac{k^2}{2M} + \omega\Upsilon - \Omega|\ell - \chi k| - V_0 + \frac{1}{\beta} \ln(2 \sinh \omega\beta), \quad (91)$$

and mean free energy takes the form

$$U = \frac{k^2}{2M} + \omega\Upsilon - \Omega|\ell - \chi k| - V_0 + \omega \coth \omega\beta. \quad (92)$$

Finally, the Massieu function under the cosmic string parameter limit  $\alpha \rightarrow 1$  is

$$f_M = \frac{k^2}{2MT} + \frac{\omega}{T} [\Upsilon - \Omega|\ell - \chi k| - V_0 + \coth \omega\beta] + k [\omega\beta \coth \omega\beta - \ln(2 \sinh \omega\beta)]. \quad (93)$$

As it can be seen, unlike the standard quantum harmonic oscillator, the thermodynamic quantities now depend, in each case, on the cosmic string parameter  $\alpha$ , the dislocation parameter  $\chi$ , and the effect of the rotational frame  $\Omega$ . This is why these parameters influence the allowed frequencies and the trajectories of the particles. There is also a dependence on angular momentum and angular velocity, which introduce corrections to the energy levels and, consequently, to the thermodynamic properties

The plots of the thermodynamic functions obtained above, their explanation and interpretation are reported in the next section for different values of the parameters  $k$ ,  $M$ ,  $\eta$ ,  $\ell$ ,  $\chi$ ,  $\omega$ , and  $\beta$ .

## 6. Plots for thermodynamic functions for the HORP

The study of the thermodynamic properties of certain quantum particles plays a crucial role in understanding quantum computing. In particular, the process of quantum storage systems involves matching a set of particles that can be described thermodynamically, this means that their properties depend on temperature, pressure and other variables. As the study of quantum systems deepens, we can better understand the behavior of these particles and how we can use them to build more powerful quantum computers.

In this Section, we plot the thermodynamic functions such as partition function, mean energy, Helmholtz free energy, entropy, specific heat and Massieu function for  $V_0 = 0$ .

Figure 1 illustrates the partition function as a function of the variable  $\alpha$ . The plot shows that as the values of  $\alpha$  increase from 0 to 0.8, there is a trend for the partition function to increase. Beyond this point, the partition function remains almost constant up to the maximum allowable value of  $\alpha$  for a specific angular frequency of 0.25. However, as the angular frequency increases to 0.50 and 0.75, the growth of the partition function decreases as  $\alpha$  increases. The same result is evident in (b) and (c). (d) When the dislocation parameter  $\chi$  is increased, a higher value of the partition function is obtained as  $\alpha$  increases.

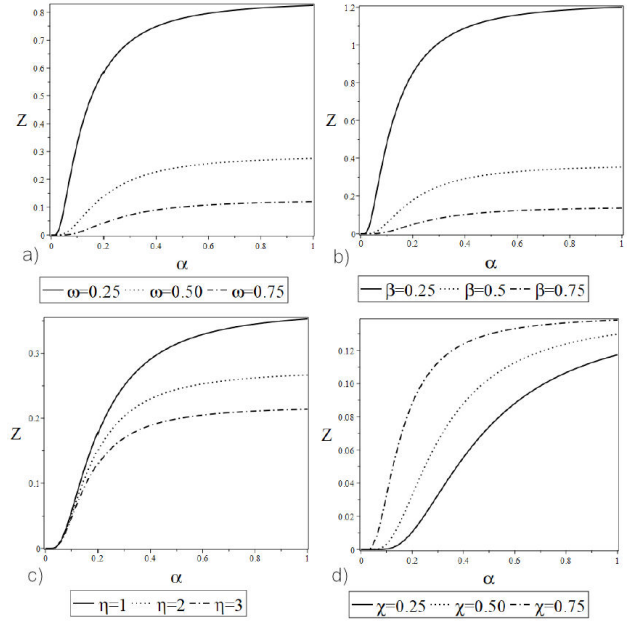


FIGURE 1. Partition function  $z$  vs cosmic string defect  $\alpha$  for some particular parameters values, a)  $k = \beta = M = \eta = \ell = 1, \chi = 0.5$ , b)  $k = \omega = M = \eta = \ell = 1, \chi = 0.5$ , c)  $k = \omega = M = \ell = 1, \beta = 0.5, \chi = 0.5$ , d)  $k = \omega = M = \ell = \eta = 1, \beta = 0.5$ .

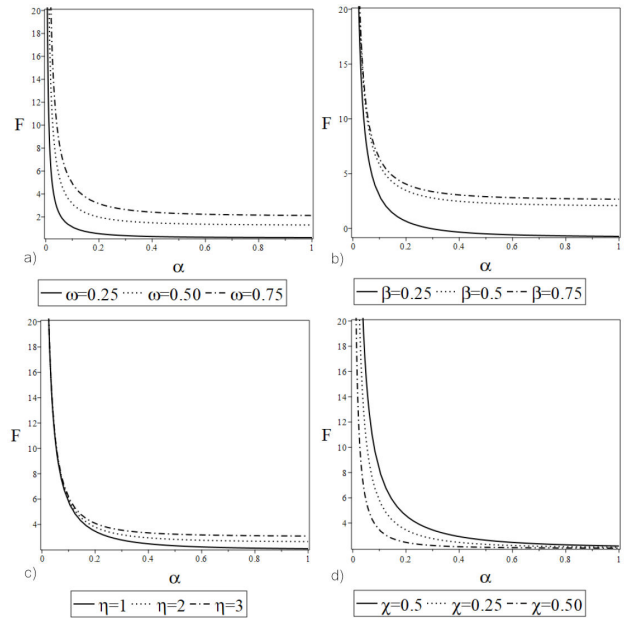


FIGURE 2. Helmholtz free energy  $F$  vs cosmic string defect  $\alpha$  for some particular parameters values a)  $k = \beta = M = \eta = \ell = 1, \chi = 0.5$ , b)  $k = \omega = M = \eta = \ell = 1, \chi = 0.5$ , c)  $k = \omega = M = \ell = 1, \beta = 0.5, \chi = 0.5$ , d)  $k = \omega = M = \ell = \eta = 1, \beta = 0.5$ .

In Fig. 2, we plot the Helmholtz free energy as a function of the variable  $\alpha$ . It can be seen that the free energy decays exponentially up to a value of about 0.2 of the parameter  $\alpha$ , from which it stabilizes at an approximately constant value for each angular frequency. It can also be observed that the decay becomes more pronounced as the angular frequency is

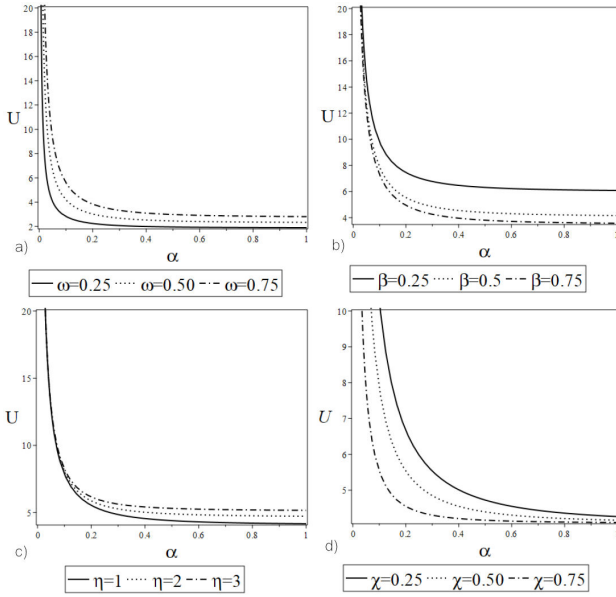


FIGURE 3. Mean free energy  $U$  vs cosmic string defect  $\alpha$  for some particular parameters values a)  $k = \beta = M = \eta = \ell = 1, \chi = 0.5$ , b)  $k = \omega = M = \eta = \ell = 1, \chi = 0.5$ , c)  $k = \omega = M = \ell = 1, \beta = 0.5, \chi = 0.5$ , d)  $k = \omega = M = \ell = \eta = 1, \beta = 0.5$ .

reduced. Similar results are obtained when the parameters  $\beta$  and  $\eta$  are varied in cases (b) and (c). In contrast, when the parameter  $\chi$  is varied, the opposite effect is observed, with greater decay for larger values of  $\chi$ .

In Fig. 3 we plot the Mean free energy as a function of the variable  $\alpha$ . (a) From this plot we can see that the Mean free energy decreases exponentially as the value of  $\alpha$  increases. Also, starting from a value of  $\alpha$  of about 0.2, it shows an almost constant behavior. As  $\omega$  decreases, the decay becomes more pronounced. b) In this case, the decay is exponential, similar to that observed in case a). The only difference is that the decay is more pronounced when  $\beta$  is larger. c) This case also shows an exponential decay similar to that observed in case a), but with a modified  $\eta$  parameter. d) We observe that the larger the  $\chi$  parameter, the faster exponential decay occurs with the same characteristics as in the previous cases.

Figure 4 shows the entropy as a function of the angular frequency  $\omega$ . a) Shows the exponential decay of the entropy

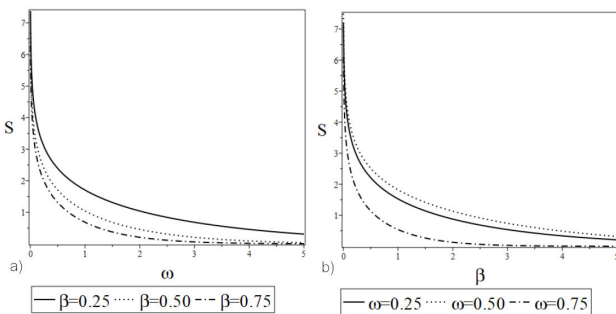


FIGURE 4. a) The Entropy  $S$  vs  $\omega$  for  $k = 1$ , b) The Entropy  $S$  vs  $\beta$  for the parameter  $k = 1$ .

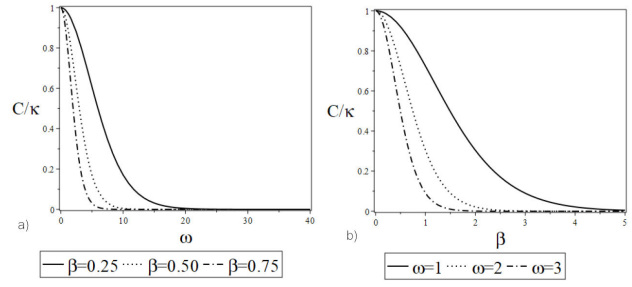


FIGURE 5. a) Specific heat capacity  $C/k$  vs  $\omega$  for different values of the parameters  $\beta$ , b) Specific heat capacity  $C/k$  vs  $\beta$  for different values of the parameters  $\omega$ .

as the value of  $\omega$  is varied. For a value of  $\omega = 4.5$  the entropy is almost constant. It can also be observed that the decay becomes more pronounced as the value of the parameter  $\beta$  increases. b) In this case, an exponential decay can be seen as the value of the parameter  $\beta$  increases. The entropy reaches an almost constant value when  $\beta = 4.5$ . It can also be seen that the decay becomes more pronounced as  $\omega$  is increased.

Figure 5 presents a plot of the specific heat as a function of angular frequency. a) It illustrates an exponential decay as the angular frequency increases. It can be seen that for a value of  $\beta = 0.75$ , the specific heat becomes zero for a value of  $\omega = 10$  approximately, and something similar occurs when  $\beta = 0.50$ . However, for  $\beta = 0.25$ , it becomes zero up to  $\omega = 20$ , with a steeper drop observed for larger values of  $\beta$ . b) The plot illustrates a clear decrease as  $\beta$  increases, with a greater intensity in its decay observed for larger values of  $\omega$ . Furthermore, the specific heat becomes zero at a value of approximately  $\beta = 2$ , for  $\omega = 3$ , at  $\beta = 2.5$ , for  $\omega = 2$  and for  $\omega = 1$  it becomes zero up to a value of  $\beta = 4.5$ .

Figure 6 shows the Massieu function as a function of absolute temperature. a) As the absolute temperature increases, an asymptotic exponential decay is observed. Around  $T = 40$ , a constant behavior is observed. This plot shows that the decay is more pronounced at higher values of  $\beta$ . b) As  $T$  increases, an exponential decay is observed, which is more pronounced for lower values of  $\eta$ . c) As  $T$  increases, a decay is observed, which is more pronounced for higher values of  $\omega$ , with a constant behavior around  $T = 50$ . d) As  $T$  increases, an asymptotic exponential decay is observed, and for small values of  $\ell$ , the decay is more pronounced.

Figure 7 we plot the partition function as a function of the variable  $\alpha$ . a) In this plot, it is observed that the partition function tends to increase as the values of  $\alpha$  increase between 0 and 0.1. In this case, when the parameter  $\chi = 0$ , there are no indications of constant behavior up to the maximum allowed value for  $\alpha$ . Moreover, when the angular frequency increases from 0.25 to 0.75, the growth rate of the partition function decreases. b) The description is similar to that given in case a), except that in this case the growth rate of the partition function decreases as  $\beta$  increases. c) The behavior in this plot is similar to that described in case a), but in this case, we modify the value of  $\eta$  and deduce that the lower the value

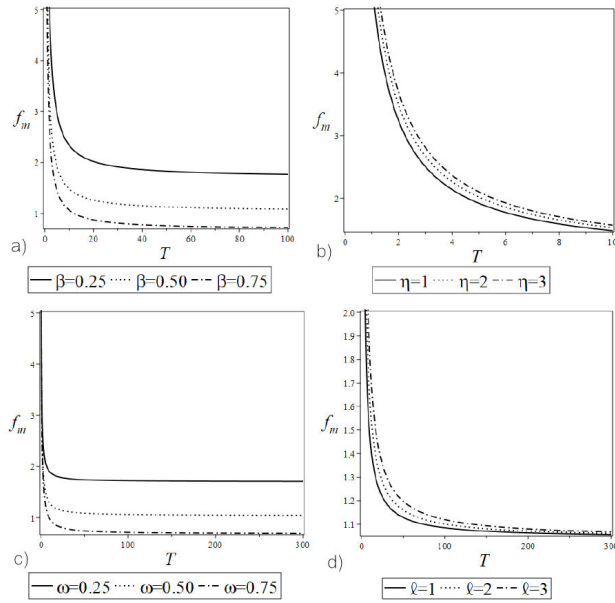


FIGURE 6. The Massieu function  $f_m$  vs absolute temperature  $T$  for some particular parameters values, a)  $k = \beta = \alpha = M = \eta = \ell = 1, \chi = 0.5$ , b)  $k = \alpha = M = \ell = \eta = \beta = 1, \alpha = 0.5\chi = 0.5$ , c)  $k = M = \eta = \beta = \ell = 1, \alpha = 0.5, \chi = 0.5$ , d)  $k = \omega = M = \eta = 1, \alpha = 0.5, \beta = 0.5$ .

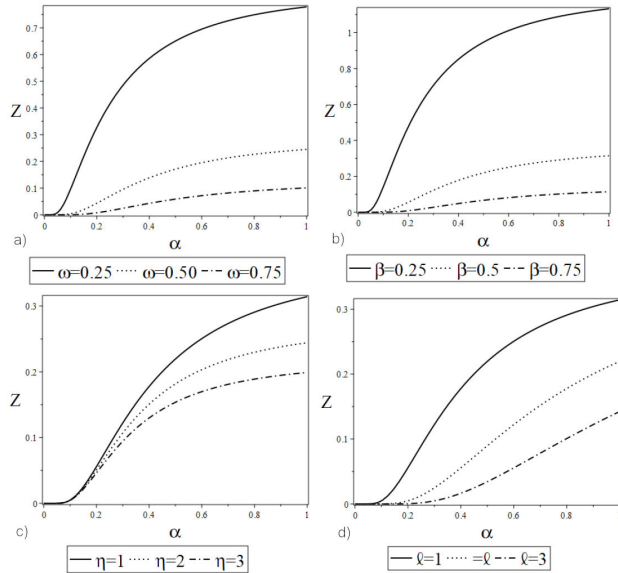


FIGURE 7. Partition function  $z$  vs cosmic string defect  $\alpha$  for different parameters values a)  $k = \beta = M = \eta = \ell = 1$ , b)  $k = \omega = M = \eta = \ell = 1$ , (c)  $k = \omega = M = \ell = 1, \beta = 0.5$ , d)  $k = \omega = M = \eta = 1, \beta = 0.5$ .

of this parameter, the higher the growth rate of the partition function. d) In this case, the partition function increases as  $\alpha$  increases. It is also observed that the lower the value of the parameter  $\ell$ , the greater the increase in the partition function. The growth rate of the partition function decreases for cases a), b), and c) with respect to  $\alpha$  when  $\chi \neq 0$ .

In Fig. 8 we plot the Helmholtz free energy as a function of the variable  $\alpha$ . a) An asymptotic exponential decay of this

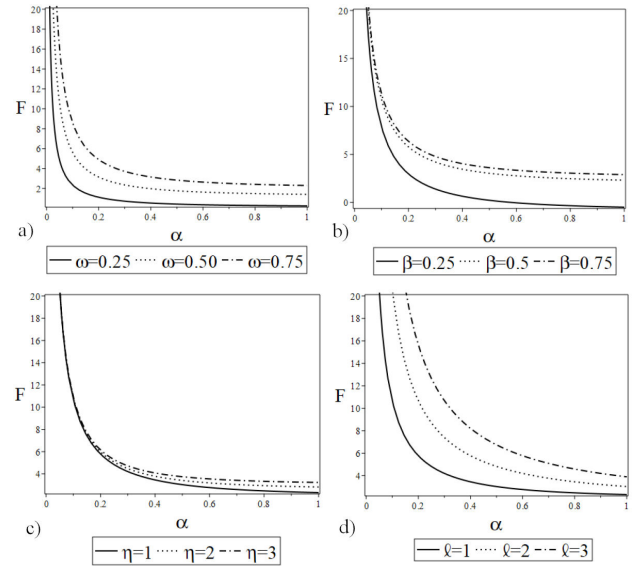


FIGURE 8. Helmholtz free energy vs cosmic string defect  $\alpha$  for some particular parameters values a)  $k = M = \eta = \ell = \beta = 1$ , b)  $k = \omega = M = \eta = \ell = 1$ , c)  $k = \omega = M = \ell = 1, \beta = 0.5$ , d)  $k = \omega = M = \eta = 1, \beta = 0.5$ .

energy is observed as the value of  $\alpha$  increases. This decay is more pronounced for smaller values of the angular frequency  $\omega$ . b) In this case, the description is similar to that in a), except that the decrease in the value of the energy is smaller as the value of  $\beta$  increases. c) The behavior in this plot is similar to that described in a), but in this case, we modify the value of  $\eta$ , and we notice that the smaller the value of this parameter, the faster the energy decreases. d) In this case, an exponential decay is observed. As the value of the parameter  $\ell$  decreases, there is a greater reduction in the energy values. The rate of decrease of the Helmholtz energy is slower for cases a), b), and c) with respect to  $\alpha$  than in the case with  $\chi \neq 0$ .

In Fig. 9 we plot the Mean free energy as a function of the variable  $\alpha$ . (a) An asymptotic exponential decay in the energy can be observed as the value of  $\alpha$  increases. There is a more pronounced decay for smaller values of the angular frequency  $\omega$ , and it seems to approach to constant values for an  $\alpha$  value of approximately 0.9. (b) Similarly, an exponential decay is observed as  $\alpha$  increases. In this case, the decay is more pronounced as  $\beta$  increases. (c) The behavior in this plot is similar to that described in (a), but in this case, we modify the value of  $\eta$ , and we notice that the smaller the value of this parameter, the faster the energy decays. (d) Once again, we observe an exponential decay similar to the previous three cases. As the value of the parameter  $\ell$  decreases, there is a greater reduction in the energy values. The rate of decrease of the average energy is slower for cases (a), (b), and (c) with respect to  $\alpha$  than in the case with  $\chi \neq 0$ .

In Fig. 10 we plot the Massieu function as a function of absolute temperature. a) This plot shows an asymptotic exponential decay. It can be observed that starting from a value close to  $T = 50$ , the Massieu function exhibits approximately constant behavior. This plot also shows that for larger values

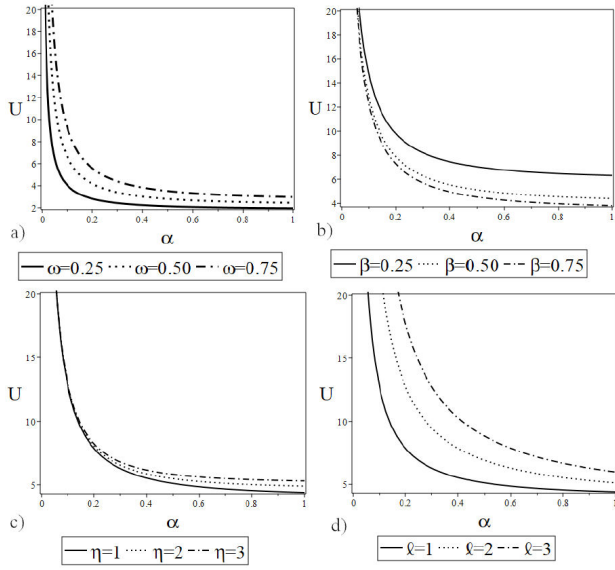


FIGURE 9. Mean free energy  $U$  vs cosmic string defect  $\alpha$  for some particular parameters values a)  $k = \beta = M = \eta = \ell = 1, \chi = 0.5$ , b)  $k = \omega = M = \eta = \ell = 1, \chi = 0.5$ , c)  $k = \omega = M = \ell = 1, \chi = \beta = 0.5$ , d)  $k = \omega = M = \eta = 1, \chi = \beta = 0.5$ .

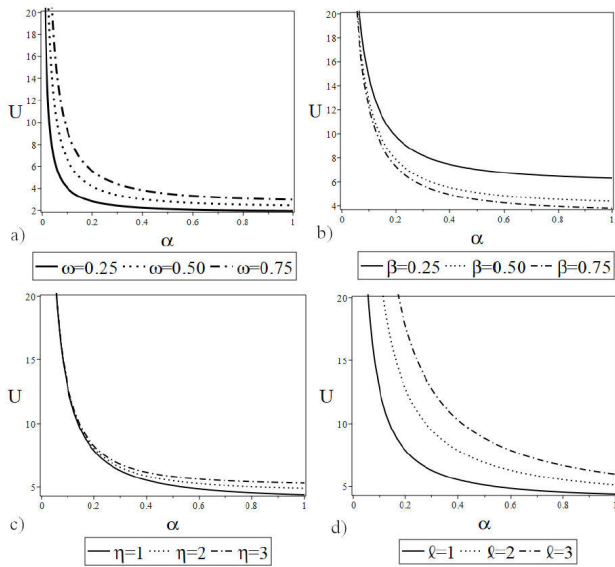


FIGURE 10. The Massieu function  $f_m$  vs the absolute temperature  $T$  for some particular parameters values a)  $k = \omega = M = \eta = \ell = 1, \alpha = 0.5$ , b)  $k = M = \ell = \eta = \omega = \ell = 1, \alpha = \beta = 0.5$ , c)  $k = M = \eta = \beta = \ell = 1, \alpha = 0.5$ , d)  $k = \omega = M = \eta = \beta = 1, \alpha = 0.5, \beta = 0.5$ .

of the parameter  $\beta$ , the decay is more pronounced. b) An exponential decay of the function is observed as  $T$  increases. In this case, the decay is slightly more pronounced as  $\eta$  decreases. c) Once again, we observe an asymptotic decay, the increasing the value of the parameter  $\omega$  leads to a greater reduction in the values of this function. d) An exponential decay is observed in this case as the value of the absolute temperature increases. A more pronounced decay is observed as

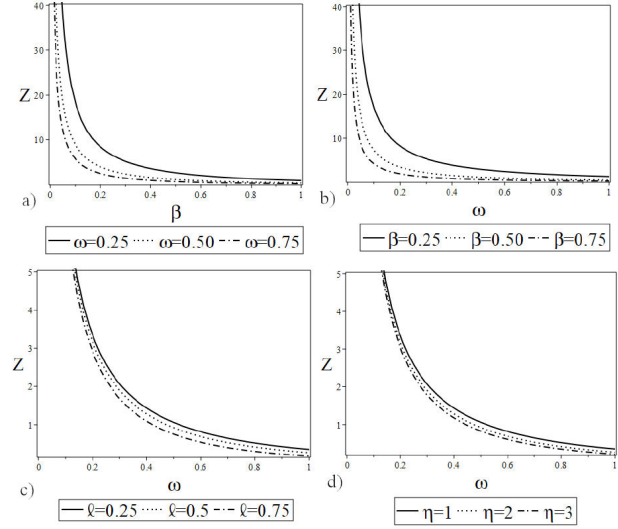


FIGURE 11. a) Partition function  $z$  vs  $\beta$  for the parameters values  $k = M = \eta = \ell = 1, \chi = 0.5$ , b) Partition function  $z$  vs  $\omega$  for the parameters values  $k = M = \eta = 1, \chi = \beta = 0.5$ , c) Partition function  $z$  vs  $\beta$  for the parameters values  $k = \omega = M = \ell = 1, \beta = \chi = 0.5$ , d) Partition function  $z$  vs  $\beta$  for the parameters values  $k = \omega = M = \ell = 1, \chi = \beta = 0.5$ .

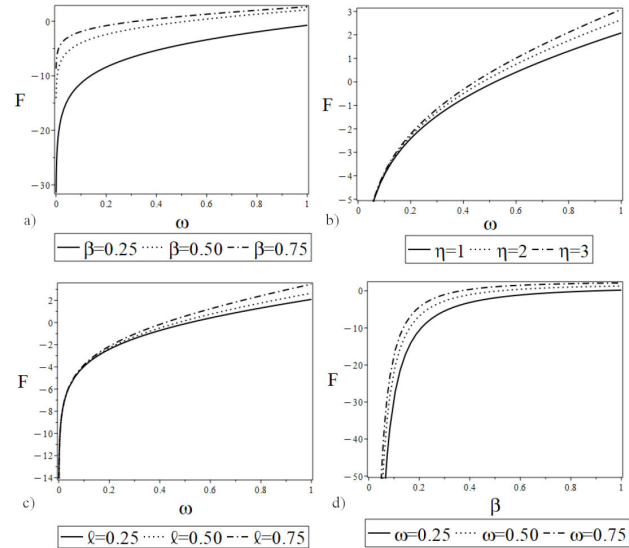


FIGURE 12. a) Helmholtz free energy  $f_m$  vs  $\beta$  for the parameters values  $k = M = \eta = \ell, \chi = 0.5$ , b) Helmholtz free energy  $f_m$  vs  $\omega$  for the parameters values  $k = M = \eta = \ell = 1, \chi = 0.5$ , c) Helmholtz free energy  $f_m$  vs  $\omega$  for the parameters values  $k = M = \ell = 1, \chi = \beta = 0.5$ , d) Helmholtz free energy  $f_m$  vs  $\omega$  for the parameters values  $k = \omega = M = \eta = 1, \chi = \beta = 0.5$ .

the value of  $\ell$  decreases. The rate of decay is similar to the case with  $\chi \neq 0$ , but for b), the decay occurs at a higher value of  $T$ .

In Fig. 11a) This plot shows that the partition function decays exponentially as  $\beta$  increases. It can be observed that starting at an approximate value of  $\beta = 0.9$ , this function appears to behave in a roughly constant manner. It is also noted that for larger values of  $\omega$ , the decay is more pronounced.

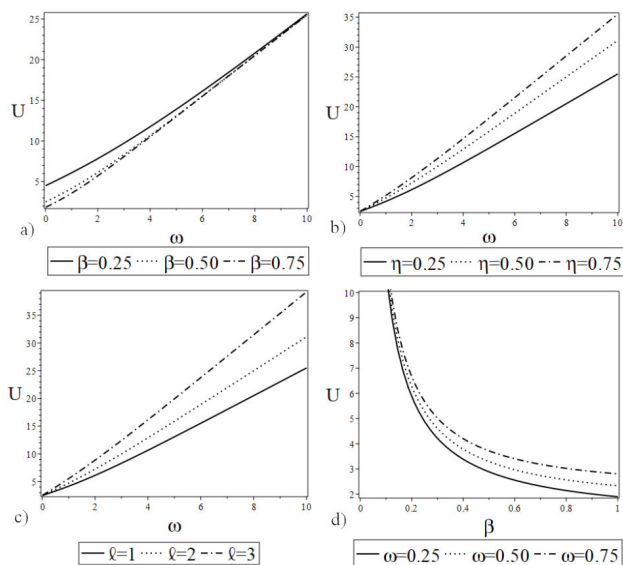


FIGURE 13. a) Mean free energy  $U$  vs  $\omega$  for the parameters values  $k = M = \eta = \ell = 1, \chi = 0.5$ , b) Mean free energy  $U$  vs  $\beta$  for the parameters values  $k = M = \eta = \ell = 1, \chi = 0.5$ , c) Mean free energy  $U$  vs  $\omega$  for the parameters values  $k = M = \ell = 1, \chi = \beta = 0.5$ , d) Mean free energy  $U$  vs  $\omega$  for the parameters values  $k = M = \eta = 1, \chi = \beta = 0.5$ .

b) In this case, the partition function is plotted as a function of the angular frequency, showing an exponential decay and approximately constant behavior starting from a value near  $\omega = 0.9$ . Similarly, for larger values of  $\beta$ , the decay is more pronounced. c) The behavior in this plot is similar to that described in case b). We notice that for larger values of the parameter  $\ell$ , the partition function decays more significantly. d) Once again, an exponential decay is observed as the parameter  $\omega$  increases, with a greater decay as  $\eta$  becomes larger.

Figure 12a) The Helmholtz free energy is plotted as a function of the variable  $\omega$ . As  $\omega$  increases, a logarithmic increase in the energy is observed. The increase is more pronounced for higher values of  $\beta$ . b) In this case, the growth continues as  $\omega$  increases. The increase is slightly more pronounced for higher values of the parameter  $\eta$ . c) A logarithmic growth is observed as  $\omega$  increases. The energy increases as the value of  $\ell$  increases. d) An asymptotic logarithmic growth is observed as the value of  $\beta$  increases. This growth is accentuated with increasing the angular frequency.

Figure 14a) The Massieu function is plotted as a function of absolute temperature  $T$ . An asymptotic exponential decay is observed. The function exhibits an approximately constant behavior from a value close to  $T = 50$ . This plot also reveals that for higher values of the parameter  $\beta$ , the decay is more pronounced. b) This plot shows an exponential decay of the function as  $T$  increases. It can be seen that the decay becomes slightly more pronounced as  $\eta$  decreases. c) An asymptotic exponential decay is observed as  $T$  increases. When the parameter  $\omega$  increases, a greater reduction in the values of this function occurs. d) In this case, an exponential decay is observed as the absolute temperature value increases. The de-

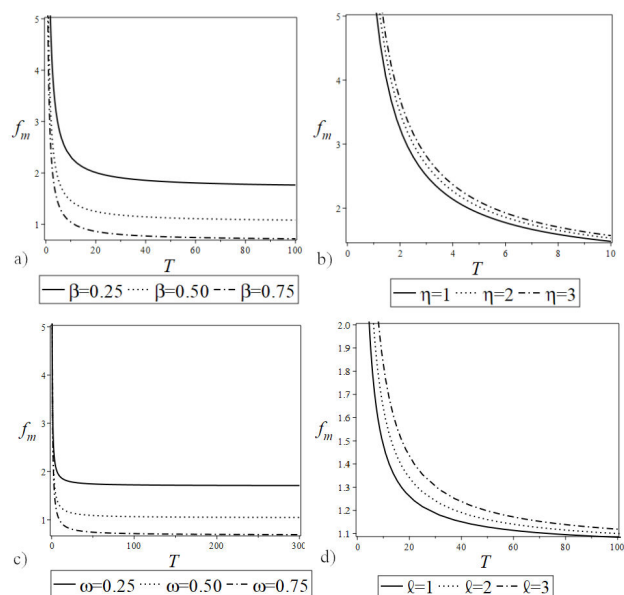


FIGURE 14. The Massieu function  $f_m$  vs the absolute temperature  $T$  for the parameters values a)  $k = \omega = M = \eta = \ell = 1, \chi = 0.5$ , b)  $k = M = \omega = \ell = \eta = \ell = 1, \alpha = \chi = \beta = 0.5$ , c)  $k = M = \eta = \beta = \ell = 1, \chi = 0.5$ , d)  $k = \omega = M = \eta = \ell = 1, \chi = 0.5, \beta = 0.5$

ca) becomes somewhat more pronounced as the value of  $\ell$  decreases. For this case, the behaviors of the functions are similar to those in scenarios involving cosmic strings and dislocation parameters.

## 7. Concluding remarks

In this paper, we have used an algebraic approach to investigate a quantum harmonic oscillator in the cosmic string space-time that contains a dislocation, given by Eq. (1), plus the presence of a repulsive square-inverse potential. We applied the Schrodinger factorization method to the second order differential equations obtained in Ref. [21]. This allowed us to obtain the generators of the  $su(1, 1)$  algebra. Using the theory of unitary representations for this algebra, we were able to obtain the energy spectrum and the eigenfunctions for this problem. Proceeding exactly in the same way, we study the harmonic oscillator plus a repulsive inverse-square potential within the same cosmic string space-time and we obtained the energy spectrum and the eigenfunctions.

Furthermore, we constructed the Perelomov coherent states for both cases from the Sturmian basis of the  $su(1, 1)$  Lie algebra for both cases, *i.e.* the quantum harmonic oscillator in the presence of a repulsive quadratic inverse potential within a cosmic string space-time containing a dislocation and the one containing a rotational reference frame. Also, for both cases, we found their corresponding coherent states and its time evolution in a closed form.

Moreover, for each of the problems studied in the present paper, we have calculated and plotted the thermodynamic functions such as the partition function, the Helmholtz free

energy, the mean free energy, the entropy, the specific heat capacity and the Massieu function.

Finally, the results we found are particularized and plotted for zero dislocation parameter  $\chi \rightarrow 0$  and for no cosmic string  $a \rightarrow 1$  for the energy spectra, the eigenfunctions, the coherent states and their time evolution, and the thermodynamic properties.

## Appendix

### A. The $SU(1, 1)$ Group and its coherent states

In the context of Lie algebra theory, the  $su(1, 1)$  algebra is defined by three generators,  $\mathcal{L}_\pm$  and  $\mathcal{L}_0$ , which satisfy the following commutation relations [58]

$$[\mathcal{L}_0, \mathcal{L}_\pm] = \pm \mathcal{L}_\pm, \quad [\mathcal{L}_-, \mathcal{L}_+] = 2\mathcal{L}_0. \quad (\text{A.1})$$

The action of the above operators in the Fock space states  $\{|k, n\rangle, n = 0, 1, 2, \dots\}$ , is defined according to the existing literature, as

$$\mathcal{L}_+|k, n\rangle = \sqrt{(n+1)(2k+n)}|k, n+1\rangle, \quad (\text{A.2})$$

$$\mathcal{L}_-|k, n\rangle = \sqrt{n(2k+n-1)}|k, n-1\rangle, \quad (\text{A.3})$$

$$\mathcal{L}_0|k, n\rangle = (k+n)|k, n\rangle, \quad (\text{A.4})$$

$$C^2|k, n\rangle = k(k-1)|k, n\rangle. \quad (\text{A.5})$$

These operators establish the theory of unitary irreducible representations of the Lie algebra  $su(1, 1)$ , where  $|k, 0\rangle$  is the lowest normalized state.

Now, in terms of the displacement operator  $D(\xi)$ , it is known that the  $SU(1, 1)$  Perelomov coherent states  $|\zeta\rangle$  are defined as

$$|\zeta\rangle = D(\xi)|k, 0\rangle, \quad (\text{A.6})$$

here  $D(\xi) = \exp(\xi\mathcal{L}_+ - \xi^*\mathcal{L}_-)$  and  $\xi$  is a complex number. It can be shown that the displacement operator has the following property from the fact that  $\mathcal{L}_+^\dagger = \mathcal{L}_-$  and  $\mathcal{L}_-^\dagger = \mathcal{L}_+$

$$D^\dagger(\xi) = \exp(\xi^*K_- - \xi K_+) = D(-\xi). \quad (\text{A.7})$$

The normal form of the displacement operator is written as

$$D(\xi) = \exp(\zeta\mathcal{L}_+) \exp(\eta\mathcal{L}_0) \exp(-\zeta^*\mathcal{L}_-), \quad (\text{A.8})$$

where  $\xi = -(1/2)\tau e^{-i\varphi}$ ,  $\zeta = -\tanh([1/2]\tau)e^{-i\varphi}$  and  $\eta = -2 \ln \cosh |\xi| = \ln(1 - |\zeta|^2)$  [57]. Therefore, by using Eq. (A.8) and Eqs. (A.2)-(A.4), The Perelomov coherent states can be written as follows [54]

$$|\zeta\rangle = (1 - |\xi|^2)^k \sum_{s=0}^{\infty} \sqrt{\frac{\Gamma(n+2k)}{s!\Gamma(2k)}} \xi^s |k, s\rangle. \quad (\text{A.9})$$

### Acknowledgments

This work was partially supported by SNII-México, COFAA-IPN, EDI-IPN, SIP-IPN project number 20242284.

- 
1. T. W. B. Kibble, Some implications of a cosmological phase transition, *Phys. Rep.* **67** (1980) 183, [https://doi.org/10.1016/0370-1573\(80\)90091-5](https://doi.org/10.1016/0370-1573(80)90091-5).
  2. S. Zare, H. Hassanabadi, and M. de Montigny, Non-inertial effects on a generalized DKP oscillator in a cosmic string space-time, *Gen. Relativ. Grav.* **52** (2020) 25, <https://doi.org/10.1007/s10714-020-02676-0>.
  3. M. Barriola, and A. Vilenkin, Gravitational Field of a Global Monopole, *Phys. Rev. Lett.* **63** (1989) 341, <https://doi.org/10.1103/PhysRevLett.63.341>.
  4. E. R. Bezerra de Mello, and C. Furtado, Nonrelativistic scattering problem by a global monopole, *Phys. Rev. D.* **56** (1997) 1345, <https://doi.org/10.1103/PhysRevD.56.1345>.
  5. Ti-Sheng, Chen, *et al.*, Pseudospin symmetry in relativistic framework with harmonic oscillator potential and Woods-Saxon potential, *Chinese physics letters.* **20.3** (2003) 358, <https://doi.org/10.1088/0256-307X/20/3/312>.
  6. P. Exner, Complex-potential description of the damped harmonic oscillator, *Journal of Mathematical Physics.* **24.5** (1983) 1129, <https://doi.org/10.1063/1.525840>.
  7. F. Marsiglio, The harmonic oscillator in quantum mechanics: A third way, *American Journal of Physics.* **77.3** (2009) 253, <https://doi.org/10.1119/1.3042207>.
  8. F. Ahmed, and A. Bouzenada, Quantum dynamics of spin-0 particles in a cosmological space-time, *Nuclear Physics B.* **1000** (2024) 116490, <https://doi.org/10.1016/j.nuclphysb.2024.116490>.
  9. A. Bouzenada, A. Boumali, and Edilberto O. Silva, Applications of the Klein-Gordon equation in the Feshbach-Villars representation in the non-inertial cosmic string space-time, *Annals of Physics.* **458** (2023) 169479, <https://doi.org/10.1016/j.aop.2023.169479>.
  10. F. Ahmed, and A. Bouzenada, Study of scalar particles through the Klein-Gordon equation under rainbow gravity effects in Bonnor-Melvin-Lambda space-time, *Communications in Theoretical Physics.* **76.4** (2024) 045401, <https://doi.org/10.1088/1572-9494/ad2e88>.
  11. F. Ahmed, and A. Bouzenada, Relativistic spin-0 Duffin-Kemmer-Petiau equation in Bonnor-Melvin-Lambda solution, *International Journal of Modern Physics A.* **39** (2024) 2450032, <https://doi.org/10.1142/S0217751X24500325>.
  12. F. Ahmed, and A. Bouzenada, PDM relativistic quantum oscillator in Einstein-Maxwell-Lambda space-time, **22**

- (2025) 2450253, <https://doi.org/10.1142/S0219887824502530>.
13. F. Ahmed, and A. Bouzenada, Scalar fields in Bonnor-Melvin-Lambda universe with potential: a study of dynamics of spin-zero particles-antiparticles, *Physica Scripta*. **99.6** (2024) 065033, <https://doi.org/10.1088/1402-4896/ad4830>.
  14. A. Bouzenada, *et al.*, Feshbach–Villars oscillator in Kaluza–Klein theory, *Nuclear Physics B* **994** (2023) 116288, <https://doi.org/10.1016/j.nuclphysb.2023.116288>.
  15. F. Ahmed, Aharonov-Bohm and non-inertial effects on a Klein–Gordon oscillator with potential in the cosmic string space–time with a spacelike dislocation, *Chinese Journal of Physics*. **66** (2020) 587, <https://doi.org/10.1016/j.cjph.2020.06.012>.
  16. S. Zare, H. Hassanabadi and M. de Montigny, Non-inertial effects on a generalized DKP oscillator in a cosmic string space–time, *Gen. Relativ. Gravit.* **52** (2020) 25, <https://doi.org/10.1007/s10714-020-02676-0>.
  17. A. V. D. M. Maia and K. Bakke, Harmonic oscillator in an elastic medium with a spiral dislocation, *Physica B*. **531** (2018) 213, <https://doi.org/10.1016/j.physb.2017.12.045>.
  18. A. Bouzenada, *et al.*, Dynamics of a Klein-Gordon Oscillator (KGO) in the Presence of a Cosmic String in Som-Raychaudhuri Space-Time, *Theor Math Phys*. **221** (2024) 2193, <https://doi.org/10.1134/S0040577924120134>.
  19. A. Bouzenada, A. Boumali, and F. Serdouk, Thermal properties of the 2D Klein-Gordon oscillator in a cosmic string space-time, *Theoretical and Mathematical Physics*. **216.1** (2023) 1055, <https://doi.org/10.1134/S0040577923070115>.
  20. M. M. Cunha, and Edilberto O. Silva, Relativistic Quantum Motion of an Electron in Spinning Cosmic String Spacetime in the Presence of Uniform Magnetic Field and Aharonov–Bohm Potential, *Advances in High Energy Physics*. **2021.1** (2021) 6709140, <https://doi.org/10.1155/2021/6709140>.
  21. F. Ahmed, Harmonic Oscillator in Cosmic String Space–Time with Dislocation Under a Repulsive  $1/r^2$  Potential and Rotational Frame Effects, *Few-Body Syst.* **65** (2024) 6 <https://doi.org/10.1007/s00601-023-01874-1>.
  22. R. M. Wald, Quantum field theory in curved space–time and black hole thermodynamics. (University of Chicago press, Chicago, 1994).
  23. J. R. Klauder, and Bo-Sture Skagerstam, Coherent states: applications in physics and mathematical physics. (World scientific, Singapore, 1985).
  24. R. J. Glauber, Coherent and incoherent states of the radiation field, *Physical Review*. **131.6** (1963) 2766, <https://doi.org/10.1103/PhysRev.131.2766>.
  25. G. J. Rampho, An. N. Ikot, C. O. Edet, and U.S. Okorie, Energy spectra and thermal properties of diatomic molecules in the presence of magnetic and AB fields with improved Kratzer potential, *Mol. Phys.* **119** (2021) e1821922, <https://doi.org/10.1080/00268976.2020.1821922>.
  26. C. O. Edet, P. O. Amadi, U. S. Okorie, A. Tas, A.N. Ikot, and G. Rampho, Solutions of Schrödinger equation and thermal properties of generalized trigonometric Pöschl–Teller potential, *Rev. Mex. Fis.* **66** (2020) 824, <https://doi.org/10.31349/revmexfis.66.824>
  27. C. O. Edet, U. S. Okorie, G. Osobonye, A. N. Ikot, G. J. Rampho and R. Sever, Thermal properties of Deng-Fan-Eckart potential model using Poisson summation approach, *J. Math. Chem.* **58** (2020) 989, <https://doi.org/10.1007/s10910-020-01107-4>.
  28. A. R. P. Moreira, Thermodynamic properties and entropy information of fermions in the Rindler spacetime, *Physica E*. **152** (2023) 115747, <https://doi.org/10.1016/j.physe.2023.115747>.
  29. M. Ishihara, Thermodynamics of the independent harmonic oscillators with different frequencies in the Tsallis statistics in the high physical temperature approximation, *Eur. Phys. J. B*. **95** (2022) 53, <https://doi.org/10.1140/epjb/s10051-022-00309-w>.
  30. A. Boumali, A. Bouzenada, S. Zare, and H. Hassanabadi, Thermal properties of the q-deformed spin-one DKP oscillator, *Physica A*. **628** (2023) 129134, <https://doi.org/10.1016/j.physa.2023.129134>.
  31. H. Hassanabadi, S. Sargolzaeipor and B. H. Yazarloo, Thermodynamic properties of the three-dimensional Dirac oscillator with Aharonov–Bohm field and magnetic monopole potential, *Few-Body Syst.* **56** (2015) 115, <https://doi.org/10.1007/s00601-015-0944-5>.
  32. S. H. Dong, W. H. Huang, W. S. Chung, P. Sedaghatnia and H. Hassanabadi, Exact solutions to generalized Dunkl oscillator and its thermodynamic properties, *Europhys. Lett.* **135** (2021) 30006, <https://doi.org/10.1209/0295-5075/ac2453>.
  33. A. Boumali, *et al.*, Thermal properties of the q-deformed spin-one DKP oscillator, *Physica A*. **628** (2023) 129134, <https://doi.org/10.1016/j.physa.2023.129134>.
  34. A. Boumali *et al.*, Effect of the applied electric field on the thermal properties of the relativistic harmonic oscillator in one dimension, *Ukrainian journal of physics*. **68.4** (2023) 235, <https://doi.org/10.15407/ujpe68.4.235>.
  35. M. Demirci, R. Sever, Arbitrary, Arbitrary  $\ell$ -state solutions of the Klein–Gordon equation with the Eckart plus a class of Yukawa potential and its non-relativistic thermal properties, *Eur. Phys. J. Plus*. **138** (2023) 409, <https://doi.org/10.1140/epjp/s13360-023-04030-0>.
  36. A. N. Ikot *et al.*, Relativistic and non-relativistic thermal properties with bound and scattering states of the Klein-Gordon equation for Mobius square plus generalized Yukawa, *Indian Journal of Physics*. **97.10** (2023) 2871, <https://doi.org/10.1007/s12648-023-02654-7>.
  37. A. Arda, C. Tezcan, and R. Sever, Klein-Gordon and Dirac equations with thermodynamic quantities, *Few-Body Systems*. **57.2** (2016) 93, <https://doi.org/10.1007/s00601-015-1031-7>.
  38. A. Vilenkin, Cosmic strings, *Physical Review D*. **24.8** (1981) 2082, <https://doi.org/10.1103/PhysRevD.24.2082>.

39. A. Vilenkin, A. Vilenkin, and E. P. S. Shellard, Cosmic strings and other topological defects. (Cambridge University Press, Cambridge, 1994).
40. Ch. Nayak *et al.*, Non-Abelian anyons and topological quantum computation, *Reviews of Modern Physics*. **80.3** (2008) 1083, <https://doi.org/10.1103/RevModPhys.80.1083>.
41. F. Ahmed, Effects of Cosmic String on Non-Relativistic Quantum Particles with Potential and Thermodynamic Properties, *International Journal of Theoretical Physics*. **62.7** (2023) 142, <https://doi.org/10.1007/s10773-023-05397-7>.
42. D. J. Cirilo-Lombardo, and N. G. Sanchez, Coherent states of quantum spacetimes for black holes and de Sitter spacetime, *Phys. Rev. D*. **108.12** (2023) 126001, <https://doi.org/10.1103/PhysRevD.108.126001>.
43. S. Zare, H. Hassanabadi, and G. Junker, Influences of Lorentz symmetry violation on charged Dirac fermions in cosmic dislocation space-time, *General Relativity and Gravitation* **54.7** (2022) 69, <https://doi.org/10.1007/s10714-022-02961-0>.
44. B. Boudjedaa, and F. Ahmed, Topological defects on solutions of non-relativistic equation for extended double ring-shaped potential, *Communications in Theoretical Physics*. **76** (2024) 085102, <https://doi.org/10.1088/1572-9494/ad4c5e>.
45. F. Ahmed, Hellmann potential and topological effects on non-relativistic particles confined by Aharonov-Bohm flux field, *Molecular Physics*. **121.2** (2023) e2155596, <https://doi.org/10.1080/00268976.2022.2155596>.
46. W. C. F. da Silva, K. Bakke, and R. L. L. Vitória, Non-relativistic quantum effects on the harmonic oscillator in a spacetime with a distortion of a vertical line into a vertical spiral, *The European Physical Journal C*. **79** (2019) 1, <https://doi.org/10.1140/epjc/s10052-019-7166-9>.
47. M. Salazar-Ramírez, D. Ojeda-Guillén, A. Morales-González, and V. H. García-Ortega, Algebraic solution and coherent states for the Dirac oscillator interacting with a topological defect, *Eur. Phys. J. Plus*. **134** (2019) 8, <https://doi.org/10.1140/epjp/i2019-12381-0>.
48. N. N. Lebedev, *Special Functions and their Applications*. (Dover Publications, New York, 1972).
49. L. Dantas, C. Furtado and A. L. S. Neto, Quantum ring in a rotating frame in the presence of a topological defect, *Phys. Lett. A*. **379** (2015) 11, <https://doi.org/10.1016/j.physleta.2014.10.016>.
50. R. L. L. Vitória and K. Bakke, Rotating effects on the scalar field in the cosmic string spacetime, in the spacetime with space-like dislocation and in the spacetime with a spiral dislocation, *The European Physical Journal C*. **78** (2018) 1, <https://doi.org/10.1140/epjc/s10052-018-5658-7>.
51. K. Bakke, Rotating effects on the Dirac oscillator in the cosmic string spacetime, *General Relativity and Gravitation*. **45** (2013) 1847, <https://doi.org/10.1007/s10714-013-1561-6>.
52. A. V. D. M. Maia, and K. Bakke, Topological and rotating effects on the Dirac field in the spiral dislocation spacetime, *The European Physical Journal C*. **79** (2019) 1, <https://doi.org/10.1140/epjc/s10052-019-7067-y>.
53. L.D. Landau, E.M. Lifshitz, *The Classical Theory of Fields, Course of Theoretical Physics*, vol. 2, 4th edn. (Elsevier, Oxford, 1980).
54. A. M. Perelomov, *Generalized Coherent States and Their Applications*. (Springer-Verlag, Berlin, 1986).
55. C. Cohen-Tannoudji, B. Diu, F. Laloe, *Quantum Mechanics*. (Wiley-VCH, Berlin, 1977).
56. Y. Gur, A. Mann, Radial coherent states-from the harmonic oscillator to the hydrogen atom, *Phys. At. Nucl.* **68** (2005) 1700, <https://doi.org/10.1134/1.2121919>.
57. C. C. Gerry, J. Kiefer, Radial coherent states for the Coulomb problem, *Phys. Rev. A*. **37** (1988) 665, <https://doi.org/10.1103/PhysRevA.37.665>.
58. A. Vourdas, *SU(2) and SU(1,1) phase states*, *Phys Rev. A*. **41** (1990) 1653, <https://doi.org/10.1103/PhysRevA.41.1653>.